NANOSYSTEMS:
PHYSICS, CHEMISTRY, MATHEMATICS

Kadet V.V., et al. *Nanosystems: Phys. Chem. Math.*, 2025, **16** (1), 14–21.
http://nanojournal.ifmo.ru
DOI 10.17586/2220-8054-2025-16-1-14-21

Original article

Effectiveness of the use of nanoaggregates for polymer treatment in oil fields with hard-to-recover reserves

Valeriy V. Kadet[1,a], Ivan V. Vasilev[1,b], Andrei V. Tiutiaev[1,c]

[1]Gubkin University, 119991 Moscow

[a]kadet.v@gubkin.ru, [b]vas.ivn@mail.ru, [c]tyutyaev@mail.ru

Corresponding author: V. V. Kadet, kadet.v@gubkin.ru

PACS 47.56.+r

ABSTRACT The study presents the results of comprehensive research on the efficiency of using polymer systems with nanoaggregates as oil displacement agents. Laboratory tests included experiments to determine the oil displacement coefficient on linear core models, as well as experiments to determine the oil recovery factor using parallel flow tubes of varying permeability, simulating the implementation of polymer flooding technology in stratified-heterogeneous oil-saturated reservoirs. The results of hydrodynamic studies using parallel flow tubes with polymer systems containing nanoaggregates demonstrated a significantly greater redistribution effect of filtration flows compared to traditional polymer solutions. The theoretical modeling of the polymer flooding process was conducted based on a percolation-hydrodynamic model, accounting for the specific flow characteristics of polymer systems with nanoaggregates in a porous medium. A comparison of the theoretical results with laboratory test outcomes showed good agreement.

KEYWORDS oil displacement by polymer solutions, polymer systems with nanoaggregates, oil recovery factor, percolation-hydrodynamic model, linear core models, parallel flow tubes.

FOR CITATION Kadet V.V., Vasilev I.V., Tiutiaev A.V. Effectiveness of the use of nanoaggregates for polymer treatment in oil fields with hard-to-recover reserves. *Nanosystems: Phys. Chem. Math.*, 2025, **16** (1), 14–21.

1. Introduction

Polymer flooding is one of the most widely applied chemical methods for enhancing oil recovery from reservoirs [1,2]. It increases the sweep efficiency of the reservoir treatment and significantly improves the oil recovery factor (ORF). Additionally, its broad applicability enables its implementation in reservoirs with diverse characteristics [2–5].

The primary mechanisms for improving oil recovery when polymer solutions are applied to reservoirs include:

1. *Increasing the viscosity of the displacing agent.* Adding a high-molecular-weight chemical reagent to the injected water, even at low concentrations, significantly increases the viscosity of the displacing agent. This leads to a reduction in the mobility ratio between water and oil and a more uniform displacement front.

2. *Blocking water-conducting channels.* The adsorption of polymer molecules on the surface of the pore space leads to a complete or partial blocking of conducting capillary cross-sections. Notably, the positive role of adsorption is evident in water-swept reservoirs, as it reduces water permeability and correspondingly increases oil production [1,6].

With the growing demand for developing fields with hard-to-recover reserves, the creation of new polymer systems that expand the applicability of this technology has become increasingly relevant. In recent years, significant advancements have been made in polymer composite systems with nanoaggregates, such as polymers with hyperbranched nanoaggregates (Fig. 1) [6–10]. These polymers, through the selection of functional monomers tailored to the filtration and capacitive properties (FCP) of specific reservoirs and the physicochemical properties of the fluids saturating them, provide the potential for more effective control of micro-level processes occurring during the movement of polymer systems through porous media.

The addition of nanoaggregates provides significant advantages in using such composites, including enhanced resistance to thermal and chemical degradation, more substantial viscosity increases at the same polymer concentrations, and higher oil recovery factors (ORF) compared to classical reagents (polyacrylamide and its modifications, xanthan gum, polysaccharides, etc.) [11–14].

Various modifications of crosslinked polymer gels can also serve as such composite reagents [8]. Conceptually, they can be divided into two main groups: “in situ” gel systems and preformed gels. The primary difference between these lies in the location of the gel’s three-dimensional structure formation: on the surface before injection or within the reservoir after injection. Depending on particle size, preformed gels can be categorized as macrogels (from 100 μm) or microgels (from 0.1 to 30 μm).

There are several types of microgels, including standard crosslinked, thermosensitive (Bright Water), and pH-sensitive microgels. The polymer particles of Bright Water microgel, in dry form, range in size from 0.1–1 μm and exhibit high

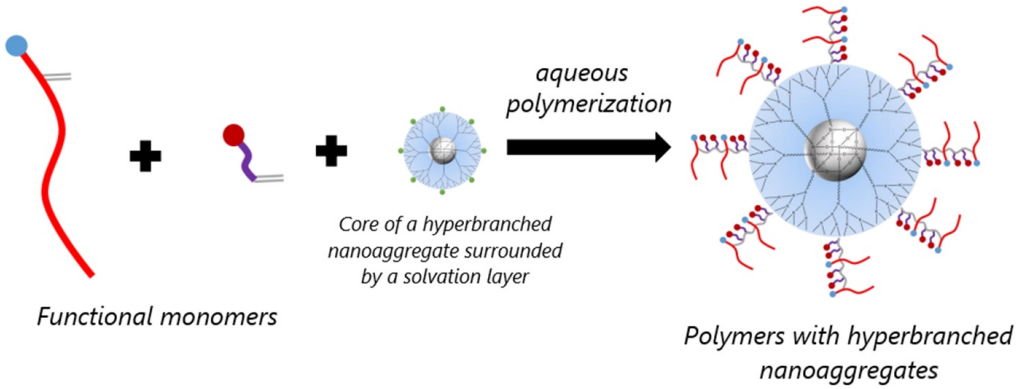

FIG. 1. Schematic of hyperbranched nanomaterial synthesis

penetration capability. Reservoir temperature triggers the process of abrupt and irreversible swelling of the particles, significantly reducing reservoir permeability. The size of the swollen particles must correspond to the characteristic pore size of the reservoir.

2. Theoretical calculation of the effect of using various polymer types

To determine the optimal parameters for implementing polymer flooding technology in oil-saturated reservoirs, the modeling process varied the FCP of the reservoir, the viscosity of the reservoir oil, and the concentration of the injected polymer solution.

To assess the effect of pore structure on the ORF, oil-saturated reservoirs with varying structures were considered: low-permeability (m_0 = 11 %, K_0 = 50 mD), medium-permeability (m_0 = 12 %, K_0 = 120 mD), and high-permeability (m_0 = 14 %, K_0 = 202 mD). The density distribution functions (DDF) of the capillaries' radii in these formations were assumed to follow a log-normal distribution (Fig. 2).

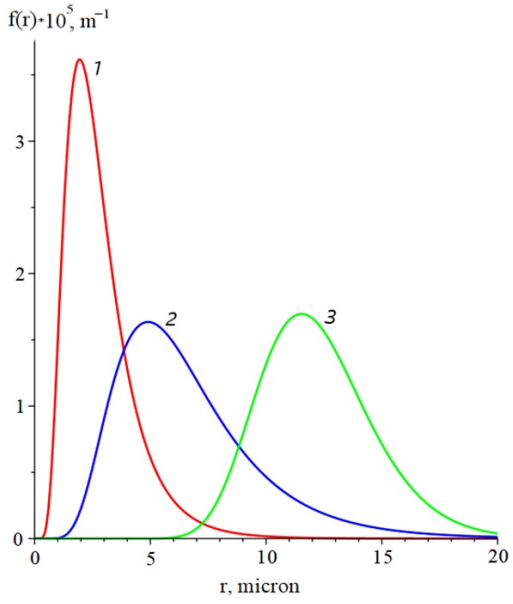

FIG. 2. Lognormal distribution density functions of capillaries by radii $f(r)$ for: 1 – Low permeability reservoir (m_0 = 11 %, K_0 = 50 mD); 2 – Medium permeability reservoir (m_0 = 12 %, K_0 = 120 mD); 3 – High permeability reservoir (m_0 = 14 %, K_0 = 202 mD)

When constructing relative phase permeability (RPP) curves based on the corresponding DDF, a percolation approach was employed [15].

The relative phase permeability curves for polymer flooding using classical polymer solutions and polymer systems with nanoaggregates are shown in Fig. 3 as solid blue lines and solid green lines, respectively. The calculated initial relative phase permeability curves for traditional flooding (without polymer addition) are presented as red dashed lines in Fig. 3.

The reduction in water-phase RPP (at water saturation S, equal to the reservoir's residual water saturation S^*) is 6 % to 16 % when using classical polymer solutions and 8 % to 21 % with polymer systems containing nanoaggregates. Notably, the greatest reduction in relative phase permeability is observed when using polymer systems with nanoaggregates in low-permeability reservoirs, reaching approximately 21 %.

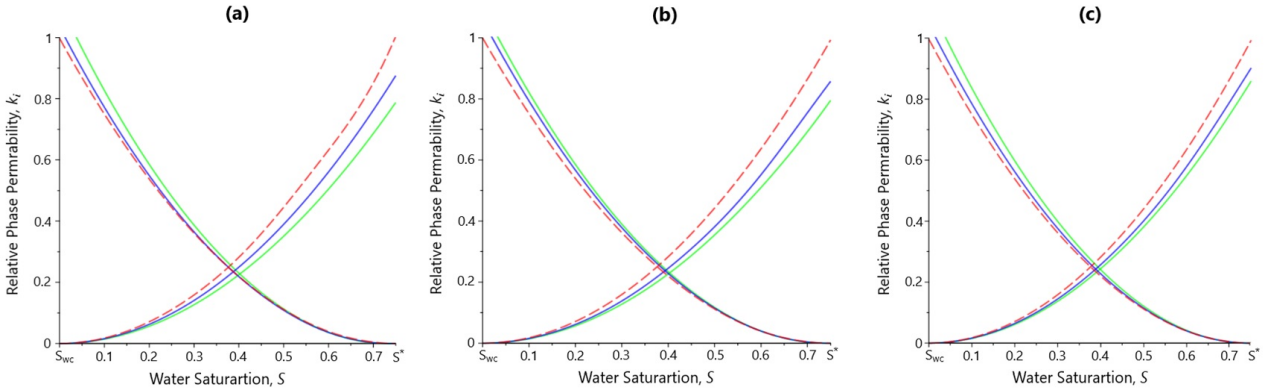

FIG. 3. Relative phase permeability curves for: (a) – high permeability reservoir; (b) – medium permeability reservoir; (c) – low permeability reservoir. Red dashed lines: basic flooding (without adding polymer); Blue solid lines: after injection of classical polymer; Green solid lines: after injection of polymer with hyperbranched nanoaggregates

The calculation of the dependence of the ORF increment relative to the baseline flooding scenario (without polymer addition) was performed by varying the concentration of the injected agent. This calculation was conducted for the case where the water cut of the produced fluid reached 99 % (Fig. 4).

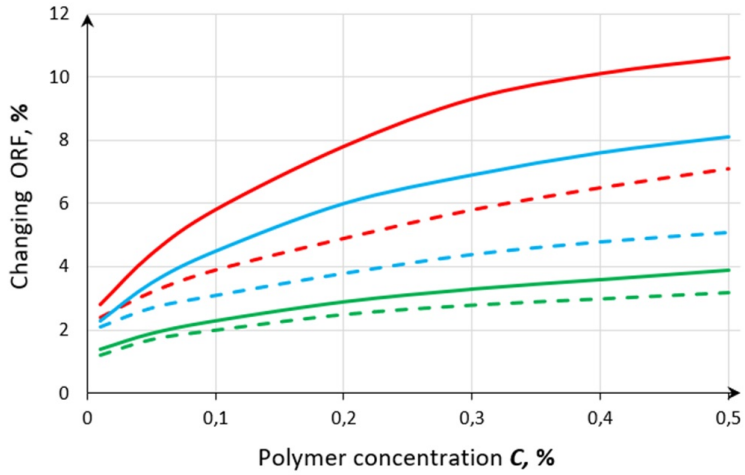

FIG. 4. Dependence of the increase in oil recovery factor relative to the basic flooding option on the concentration of the injected reagent (oil viscosity μ_0 = 50 cP) when using: polymers with hyperbranched nanoaggregates (solid lines) and classical polymer solutions (dashed lines): Red lines – Low permeability reservoir; Blue lines – Medium permeability reservoir; Green lines – High permeability reservoir

The relative increases in the oil recovery factor in various reservoirs when using polymer solutions of different types, for the most representative values of concentration and reservoir oil viscosity, are presented in Table 1.

From Table 1, it is evident that the use of polymer systems with nanoaggregates is particularly advantageous in fields with low-permeability reservoirs.

3. Laboratory Studies

Experimental research on the rheological and filtration properties of polymer systems with nanoaggregates was conducted in several stages.

For the laboratory tests, the following reagents were selected: polyacrylamide FP-107 (manufactured by SNF-CHINA) and a nanoscale reagent, chromium acetate. During polymer dissolution in water, the polyacrylamide and nanoscale additive interact at an intermolecular (nano) level, forming a crosslinked polymer system.

TABLE 1. Growth of oil recovery factor relative to the basic flooding option (without addition of polymer) at the concentration of the injected chemical reagent of 0.4 % and the viscosity of reservoir oil of 50 cP

Collector type	Increase in ORF when using classic polymer solutions, %	Increase in ORF when using polymer systems with nanoaggregates, %
Low permeability	6.5	10.1
Medium permeability	4.8	7.6
High permeability	3.1	3.5

Stage I: Solubility Study. The first stage of the research focused on the solubility of the polymer sample. Solubility is a critical parameter to consider when developing programs and plans for implementing permeability profile control technologies at specific oil fields. The solubility of a polymer in water is characterized by the rate and completeness of dissolution, which primarily depends on its molecular structure and the dispersity of the reagent powder. Achieving constant viscosity indicates the complete dissolution of the polymer.

The solubility of polymer samples was studied using a water model prepared with a specific component ionic composition. The component composition is provided in Table 2.

TABLE 2. Component composition of water

Component	HCO^{-3}	Cl^{-}	SO_4^{2-}	Ca^{2+}	Mg^{2+}	K^{+} + Na^{+}	Total concentration
Dimension	g/l	g/l	g/l	g/l	g/l	g/l	g/l
Concentration	0,204	107,262	1,008	5,127	2,164	62,789	178,550

Fig. 5 presents graphs showing the dependence of the effective viscosity of polymer solutions ($C = 0.4$ % and $C = 1$ %) on their dissolution time. The graphs indicate that the dissolution time for the majority of the reagent is 2.5 hours at $C = 0.4$ % and 3.3 hours at $C = 1$ %.

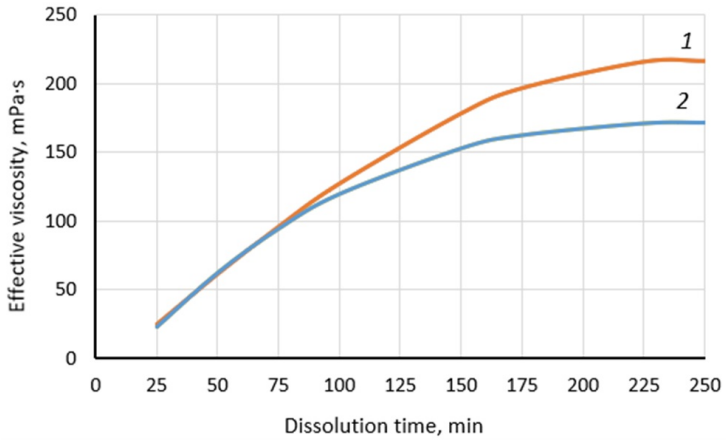

FIG. 5. Dependence of effective viscosity on dissolution time: Orange curve 1 – for polymer concentration $C = 1$ %; Blue curve 2 – for polymer concentration $C = 0.4$ %

It should be noted that under actual field conditions, the polymer dissolution time would be even shorter due to the existing pressure gradient.

Stage II: Rheological Properties Investigation. At the second stage, the rheological properties of the prepared solutions were studied using a Brookfield viscometer at a temperature of $T = 38$ ∘C, corresponding to the reservoir temperature. The investigation was conducted across a range of shear rates (0.122 – 6.12) s^{-1} (Fig. 6).

It is evident that these solutions exhibit pseudoplastic flow behavior, meaning that as the shear rate increases, the viscosity of the polymer solution decreases.

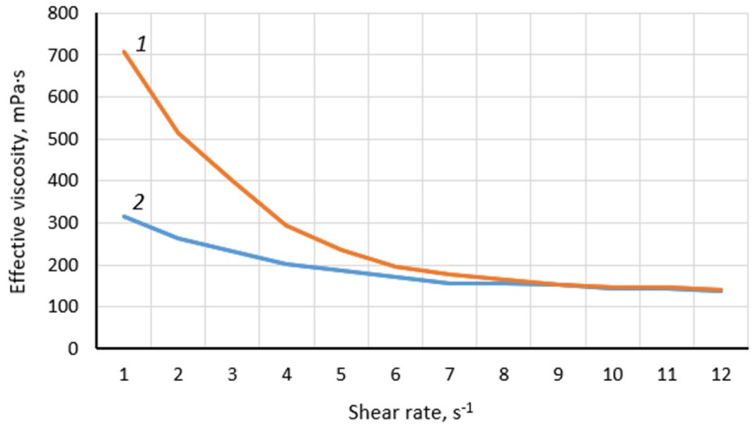

FIG. 6. Dependence of the effective viscosity of polymer solutions on the shear rate: Orange curve 1 – for polymer concentration C = 1 %; Blue curve 2 – for polymer concentration C = 0.4 %

Stage III of the experiment involved studying the kinetics of crosslinked structure formation, which is characterized by three sequential stages. In the first (initial) stage, there is a slow increase in viscosity due to the formation of microgel particles. In the second stage, the microgel particles grow larger, resulting in a more rapid increase in viscosity. Finally, in the third (final) stage, a continuous system forms throughout the volume, leading to an almost instantaneous increase in viscosity. The tested polymer, in combination with chromium acetate, demonstrated excellent structure-forming properties.

Stage IV of the experiment assessed the potential for gel formation in a porous medium through a filtration study using a single core sample. A natural core sample from the reservoir was used for this purpose (Table 3).

TABLE 3. Filtration-capacity characteristics and geometric parameters of the core sample

Rock type	Porosity, unit fraction	Absolute permeability, μm^2	Core sample length, cm	Core sample diameter, cm	Core sample volume, cm^3	Pore volume, cm^3
Sand	0.15	0.622	3.14	2.81	19.47	3.44

TABLE 4. The results of the experimental determination of the values of the displacement factor and residual oil saturation

Parameter / Experiment No.	Exp. No 1	Exp. No 2	Exp. No 3	**Exp. No 4**	**Exp. No 5**
Residual oil saturation, unit fraction.	0.318	0.312	0.288	**0.252**	**0.247**
Displacement factor, unit fraction.	0.665	0.672	0.702	**0.735**	**0.742**

The study was conducted using the automated core filtration unit UIK-4. At the beginning of the experiment, the core was saturated with injection water at a temperature of 38 ∘C, followed by the determination of water permeability. Next, a composition of 0.4 % FP-107 and 0.04 % nanoscale reagent was injected through the water-saturated core in a volume of 2 pore volumes at a filtration rate of 0.5 cm^3/min. After the injection of the composition, the core was maintained at reservoir temperature for 24 hours to enable the gel formation process. Subsequently, water was injected through the core sample again at the same volumetric rate.

Based on the experimental results, the residual resistance factor (RRF) created by the composition in the porous medium was calculated. RRF is one of the key parameters characterizing the effectiveness of the polymer flooding technology. It determines the degree of blockage of the most water-permeable filtration channels. After implementing the polymer composition with the nanosystem, the RRF was determined to be 57.3.

Stage V of the Experiment. The completeness of oil displacement by water was determined under laboratory conditions in accordance with the requirements of OST 39-195-86 [16]. The experiment was carried out using a core study setup similar to the one described in [17].

TABLE 5. Collector properties of low-permeability and high-permeability core samples during an experiment on parallel flow tubes (average values are highlighted in red)

Porosity, unit fraction	Gas permeability, μm^2	Residual oil saturation, unit fraction
Low permeability reservoir element model current tube		
0.096	0.0382	0.327
0.119	0.0429	0.321
0.097	0.043	0.310
0.111	0.0469	0.306
0.107	0.0492	0.293
0.11	0.052	0.301
0.114	0.0551	0.313
0.107	0.0557	0.279
0.125	0.0659	0.229
0.1095	**0.0486**	**0.298**
High permeability reservoir element model current tube		
0.137	0.1728	0.337
0.13	0.1738	0.335
0.133	0.1741	0.306
0.134	0.2013	0.282
0.138	0.2045	0.275
0.137	0.2124	0.275
0.136	0.2183	0.274
0.143	0.2201	0.274
0.133	0.2253	0.227
0.1355	**0.1986**	**0.287**

TABLE 6. Redistribution of filtration flows and changes in residual oil saturation after the implementation of the proposed technology

Current tube type	Ratio of volume velocities in parallel current tubes when creating residual oil saturation with produced water, unit fraction.	Ratio of volume velocities in parallel current tubes during flooding with produced water after the implementation of the proposed technology, unit fraction.	Increase in oil displacement factor, %
High permeability reservoir element model current tube	2.2	0.353	1.8
Low permeability reservoir element model current tube			9.2

The process of oil displacement by water was modeled on a composite core model assembled from 10 standard core samples obtained from the same reservoir.

Before testing, the core samples were extracted using an ethanol-benzene mixture and dried to constant weight. Then the samples were vacuum-saturated with highly mineralized formation water from the same reservoir (Table 2) and held for two days. Residual water saturation was then established in the samples by centrifugation.

The samples were subsequently saturated with kerosene and assembled into a composite reservoir model so that each subsequent sample in the displacement direction had lower permeability. The composite sample was placed in a rubber sleeve and installed in a core holder.

Next, kerosene was filtered through the linear reservoir model in a volume of about 10 pore volumes, followed by an equal amount of formation oil (a sample of which was collected from the well) at T_{res}=80 ∘C. Upon completing the oil injection, the model was held for 16 hours under thermobaric conditions corresponding to the reservoir. The initial oil saturation of the reservoir element model K_{ios} was 0.95.

The same reservoir water was used as the displacing agent. Displacement was performed at reservoir temperature (T_{res}=80 ∘C) at a constant rate until complete water breakthrough in the effluent fluid. As a result, the residual oil saturation K_{ros} was 0.318, and the displacement efficiency K_{displ} was 0.665.

After establishing residual oil saturation in the composite reservoir element model, the developed composite polymer flooding technology was implemented according to the following scheme:

(1) Oil displacement by water (without polymer addition);
(2) Injection of a well-mixed 0.4 % polymer solution;
(3) Injection of a well-mixed 1 % polymer solution;
(4) Injection of a well-mixed solution of 0.4 % polymer and 0.04 % nanoscale reagent;
(5) Injection of a well-mixed solution of 1 % polymer and 0.04 % nanoscale reagent.

Table 4 presents comparative data on the determination of residual oil saturations and displacement efficiencies for the specified scenarios.

Stage VI of the Experiment. Experiments were conducted on parallel flow tubes to study the redistribution of filtration flows and the intensification of production from low-permeability interlayers during oil recovery.

The flow tubes were composite models of reservoir elements with two interlayers differing in permeability. The displacing agent used was the formation water model specified in Table 2. Displacement was performed at reservoir temperature (T_{res}=80 ∘C) at a constant rate until the effluent fluid from the high-permeability section of the reservoir element model reached full water breakthrough.

The characteristics of the individual core samples for the low-permeability and high-permeability flow tubes are presented in Table 5.

Based on the laboratory tests, the oil displacement efficiency in the low-permeability flow tube (K_{ios} = 0.93 and K_{ros} = 0.298) was 0.679.

The oil displacement efficiency in the high-permeability reservoir element model (K_{ios} = 0.95 and K_{ros} = 0.287) was 0.698.

It is evident that the difference in displacement efficiencies between the high-permeability and low-permeability reservoir element models is negligible.

After establishing residual oil saturation in the composite reservoir element model, a thoroughly mixed 0.4 % polymer solution with the addition of 0.04 % nanoaggregate was injected. Changes in the oil volume collected in test tubes from each flow tube and the ratio of volumetric flow rates through the parallel flow tubes were recorded. The results obtained are presented in Table 6.

As shown in Table 6, the total increase in oil displacement efficiency in the parallel flow tube experiment was 11 %. This result is explained by the significant improvement in the displacement efficiency of the low-permeability flow tube due to the redistribution of filtration flows between the two flow tubes. This effect is a result of the substantial reduction in water-phase relative phase permeability in the low-permeability flow tube of the reservoir element model when polymer systems with nanoaggregates are used.

The theoretical results obtained using the percolation-hydrodynamic model (Table 1) align well with the experimental data (Table 6). Obviously, this is a consequence of the fact that the developed model fully takes into account the features of the flow of polymer solutions with included nanoaggregates, including the nature of their adsorption interaction with the surface of the pore space. At the same time, the parameters of polymer systems directly used in experiments were taken into account in the calculations. In general, this indicates a high degree of adequacy and accuracy of the constructed percolation-hydrodynamic model.

4. Conclusions

1. Experimental studies on the solubility and rheological properties of polymer composite systems were conducted. The characteristic dissolution time of the polymer composition and the establishment of a stable effective viscosity were determined. For polymer concentrations of 0.4 % and 1 % (with the addition of 0.04 % nanoaggregate in both cases),

the dissolution times were 2.5 hours and 3.5 hours, respectively. Rheological studies under varying shear rates confirmed pseudoplastic flow behavior.

2. Filtration studies were conducted on a single core sample from the selected reservoir to determine the residual resistance factor during the injection of the polymer composition (0.4 % FP-107 + 0.04 % nanoscale reagent). High RRF values indicated the formation of a stable, branched structure.

Filtration experiments on the single sample demonstrated an increase in oil recovery efficiency by (1.1–5.6) % when classical polymer solutions were used at polymer concentrations ranging from 0.4 % to 1 %. In contrast, polymer systems with nanoaggregates achieved a (10.5–11.6) % increase under the same conditions.

3. Experiments on parallel flow tubes were conducted to evaluate the efficiency of polymer flooding in oil-saturated reservoirs with stratified heterogeneity. Following the injection of a polymer composition (0.4 % FP-107 + 0.04 % nanoscale reagent), the oil displacement efficiency in the low-permeability flow tube of the reservoir element model increased by 9.2 %, while the overall model efficiency improved by 11 % relative to the baseline flooding scenario (without polymer addition).

4. Numerical studies of various polymer flooding scenarios in reservoirs of different types (considering variations in pore structure, reservoir oil viscosity, polymer type, and concentration) demonstrated a potential increase in oil recovery factor by approximately 10 % compared to the baseline flooding scenario when polymer systems with nanoaggregates were used. This estimate is consistent with the results of laboratory experiments on parallel flow tubes with different reservoir properties (low-permeability and high-permeability reservoirs).

References

[1] Zheltov Yu.P. *Development of Oil Fields: A Textbook for Universities*. Moscow, Nedra, 1986, 332 p.

[2] Zolotukhin A.B., Pyatibratov P.V., Nazarova L.N., et al. EOR methods applicability evaluation. Proceedings of the Gubkin I.M. Russian State University of Oil and Gas, 2016, **2**(283), P. 58–70.

[3] Silin M.A., Magadova L.A., Davletshina L.F., et al. Application experience and major trends in polymer flooding technology worldwide. *Territory of Oil and Gas*, 2021, **9–10**, P. 46–52.

[4] Telkov V.P., Kim S.V., Mostadjeren M. New Opportunities for Using Polymer Solutions for the Development of Heavy Oil and High-Viscosity Oil Fields. Achievements, Challenges, and Prospects for the Development of the Oil and Gas Industry: Proceedings of the International Scientific and Practical Conference Dedicated to the 60th Anniversary of Higher Oil and Gas Education in the Republic of Tatarstan, Almetyevsk, October 28–29, 2016. Almetyevsk: Almetyevsk State Oil Institute, 2016, **1**, P. 454–461.

[5] Pribylev, E. M. Analysis of world implementation experience polymer filling technologies. *Problems of the Development of Hydrocarbon and Ore Deposits*, 2020, **2**, P. 332.

[6] Kadet V.V., Vasiliev I.V. Use of hyperbranched nanocomplexes to improve the efficiency of polymer flooding. Theoretical Foundations of Chemical Engineering, 2023, **57**(6), P. 1385–1393.

[7] Grigorashchenko G.I., Zaitsev Yu.V., Kukin V.V., et al. *The Use of Polymers in Oil Recovery*. Moscow, Nedra, 1978.

[8] Ketova Iu.A., Galkin S.V., Votinov A.S., Kang W., Yang H. Analysis of the international practice in application of conformance control technologies based on cross-linked polymer gels. *Perm Journal of Petroleum and Mining Engineering*, 2020, **20**(2), P. 150–161.

[9] Tereshchenko T.A. Synthesis and application of polyhedral oligosilsesquioxanes and spherosilicates, T. A. Tereshchenko. *Polymer Science, Series B*, 2008, **50**(9-10), P. 249–262.

[10] Khavkin A.Ya. Nanophenomena and Nanotechnologies in Oil and Gas Recovery. Moscow, Izhevsk, NIC "Regular and Chaotic Dynamics", Institute for Computer Studies, 2010.

[11] Podoprigora D.G., Byazrov R.R., Khristich E.A. The current level and prospects for the development of large-volume injection technologies using polymers to increase oil recovery. *The Eurasian Scientific Journal*, 2022, **14**(2), P. 34.

[12] Seright R.S., Campbell A.R., Mozley P.S., Han P. Hydrolyzed Polyacrylamides at Elevated Temperatures in the Absence of Divalent Cations. *SPE Journal*, 2010, **15**(02), P. 341–348.

[13] Murzina L.A., Zakharova E.M., Zakharov V.P. Associative polymers to improve oil recovery. Practical Aspects of Oilfield Chemistry: Abstracts of the 4th All-Russian Scientific and Practical Conference, Ufa, May, 27–28, 2014. Ufa: OAO "BashNIPIneft", 2014, P. 17–19.

[14] Raupov I.R., Kondrasheva N.K., Raupov R.R. Development polymeric compositions for in-situ water shutoff of terrigenous deposits of oil field development. Oil and Gas Engineering, 2016, **14**(1), P. 80–87.

[15] Kadet V.V. *Percolation analysis of hydrodynamic and electrokinetic processes in porous media*. Moscow, INFRA-M, 2013, P. 139–155.

[16] OST 39-195-86. Oil. Method for Determining the Oil Displacement Factor by Water Under Laboratory Conditions.

[17] Petrov I.V., Tyutyaev A.V., Dolzhikova I.S. Program development for experimental evaluation of oil reservoir alkaline-sas floodind efficiency. *Advances in current natural sciences*, 2016, **11**, P. 182–185.

Submitted 26 December 2024; revised 16 January 2025; accepted 17 January 2025

Information about the authors:

Valeriy V. Kadet – Gubkin University, 119991 Moscow; ORCID 0000-0003-2981-5310; kadet.v@gubkin.ru

Ivan V. Vasilev – Gubkin University, 119991 Moscow; vas.ivn@mail.ru

Andrei V. Tiutiaev – Gubkin University, 119991 Moscow; tyutyaev@mail.ru

Conflict of interest: the authors declare no conflict of interest.